9th International Congress of Croatian Society of Mechanics
18-22 September 2018
Split, Croatia

The Characteristics of 2D and 3D Modelling Approach in Calibration of Reinforced Concrete Frames Cyclic Behaviour

Filip ANIĆ[*], Davorin PENAVA[*], Dmitrii LEGATIUK[+], Lars ABRAHAMCZYK[+], Uwe KÄHLER [‡]

**** Josip Juraj Strossmayer University of Osijek, Faculty of Civil Engineering Osijek, 3 Vladimir Prelog Street, HR-31000 Osijek, Croatia***
E-mails: {filip.anic, davorin.penava}@gfos.hr

[+]Bauhaus-Universität Weimar, Earthquake Damage Analysis Center & Institut für Angewandte Mathematik, Marienstraße 7A & Coudraystraße 13B, D-99421 Weimar, Germany
E-mail: {dmitrii.legatiuk, lars.abrahamczyk} @uni-weimar.de

[‡]Universidade de Aveiro, Departamento de Matemática, 3810-193 Aveiro, Portugal
E-mail: ukaehler@ua.pt

Abstract. *A 3D FE micromodel of a bare RC frame was developed. The model is based on validated 2D micromodel. The 3D model obtained higher response when compared to its 2D counterpart. Consequently, a calibration of the frame was initiated. Calibration involved modifying parameters that govern the plastic behaviour of the computational model, such as fracture energy, plastic displacement and direction of plastic flow. It was shown that the greatest effect in lowering the response had the direction of plastic flow. Plastic flow direction was selected as -0.1 as it has greatest correlation with the experimental data. Negative value denotes that material volume will decrease due to crushing.*

1 Introduction

During earthquakes ground motion, high rise structures such as reinforced concrete (RC) frames with masonry infill / panels are excited both in in-plane (IP) and out-of-plane (OoP) manner. The interaction between the frame and infill can be considered complex, which led engineers to design frames and walls separately. Consequently, in the last decade, this resulted in numerus studies that divided the problem onto the load acting manner: 1. IP; 2. OoP; 3. IP+OoP & OoP+IP loading. The majority of research was done in IP field [1], [2], and presently, the OoP field is starting to grow.

This paper is a part of OoP studies on masonry infilled RC frames, a common building practice in South Europe [3]. A numerical study is to be carried out to asset the oncoming experiments. Accordingly, the bare frame model should be calibrated firstly. The micromodel is calibrated on experimental IP cyclic, quasi-static results from [4] (Figure 1). Once calibrated, bare frame model can be considered calibrated in OoP direction as well. Furthermore, the bare frame model will be used for IP calibration of infilled frames given by [4].

Frame was designed as medium ductility class (DCM) as designated by EN 1998-1-1 [5] and EN 1992-1-1 [6] provisions. Furthermore, frame was scaled to the ratio of 1:2.5.

The 3D micromodel presented here is based on 2D micro model developed by [7]. However, during the analysis the 3D model obtained stronger response than its 2D counterpart (Figure 2). From Figure 2 it is evident that behaviour is approximately the same for both models up until reaching yielding point. Therefore, this paper presents the calibration of the 3D bare frame micromodel with variations of numerical material model parameters that govern the plastic and cracks behaviour. Both 2D and 3D micromodels were created in Atena 2D and 3D finite element (FE) software [8] respectively.

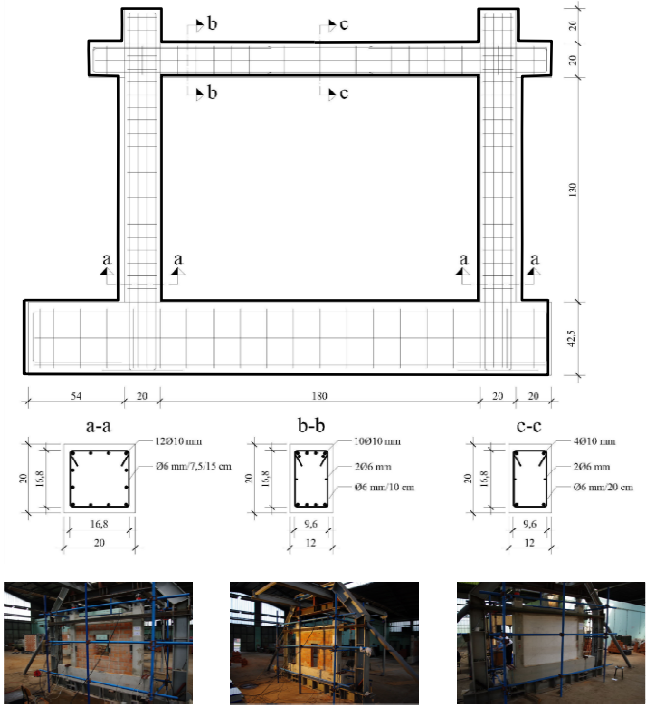

Figure 1: Reinforcement design upper; tested infilled frames lower [4]

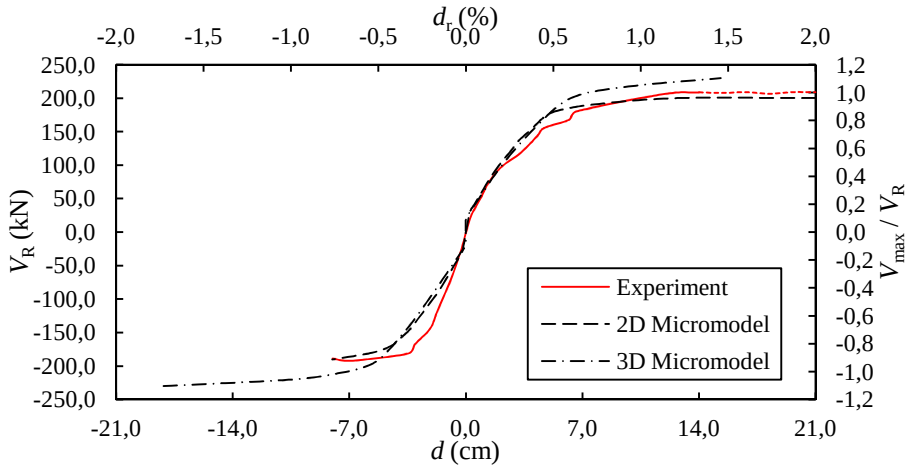

Figure 2: 2D vs. 3D Micromodel approach

2 Materials and Methods

2.1 Numerical Materials

The material model used for describing concrete's behaviour is presented in Table 1. Rebar properties are modelled with bilinear law, and is presented in Table 2 The values for both Table 1 & 2 are obtained from [7] and they are based on small scale experimental and calculated findings [9]. The nonlinear (NL) spring function represents the friction of rollers due to high axial forces to the columns. For more insight about the NL spring please refer to [10] paper.

Table 1: CC Nonlinear Cementitious 2 numerical model properties

Description	Symbol	Frame concrete	Unit
Elastic modulus	E	4.100E+04	MPa
Poisson's ratio	μ	0.200	/
Tensile strength	f_t	4.000	MPa
Compressive strength	f_c	-5.800E+01	MPa
Specific fracture energy (Eq.1)	G_f	1.200E-04	MN/m
Crack spacing	s_{max}	0.125	m
Tensile stiffening	c_{ts}	0.400	/
Critical compressive disp.	W_d	-1.000E-03	/
Plastic strain at f_c	ε_{cp}	-1.417E-03	/
Reduction of f_c due to cracks	$r_{c.lim}$	0.800	/
Crack shear stiffness factor	S_F	2.000E+01	/
Aggregate size		1.600E-02	m
Fixed crack model coefficient		0.000	/

2.2 Modifications to the Numerical Models

As stated in introduction, due to differences in the plastic region of 2D & 3D approach, the calibration was set to parameters that govern the plastic behaviour of the computational model.

Fracture energy G_F determines the materials resistance to crack propagation [11]. Fracture energy was not tested experimentally, rather, it calculated based upon concretes mechanical properties using Eq. 1 as recommended by [12]. Consequently, different approaches of calculating fracture energy G_F (Eq. 1-6) were examined. Equations 2 – 6 are obtained from [13]. Calculated values with differences in respect to Eq. 1 are presented in Table 3. The values of calculated G_F vary from -30% to 14% (Table 3).

$$G_F = 0.000025\, f_t \tag{1}$$

$$G_F = G_{F0}\left(\frac{f_{cm}}{f_{cmo}}\right) \tag{2}$$

$$G_F = G_{F0}\ln\left(1+\frac{f_{cm}}{f_{cmo}}\right) \tag{3}$$

$$G_F = G_{F0}\ln\left(1-0.77\frac{f_{cm}}{f_{cmo}}\right) \tag{4}$$

$$G_F = G_{F0}\left(\frac{f_{cm}}{f_{cmo}}\right)^{0.18} \tag{5}$$

$$G_F = 73 f_{cm}^{\ 0.18} \tag{6}$$

Table 2: Bilinear steel reinforcement material properties

Description		Value	Unit
Elastic modulus	E	2.10 E+05	MPa
Yield strength	σ_y	5.50 E+02	MPa
Tensile strength	σ_t	6.50 E+02	MPa
Limited ductility of steel	ε_{lim}	0.01	/

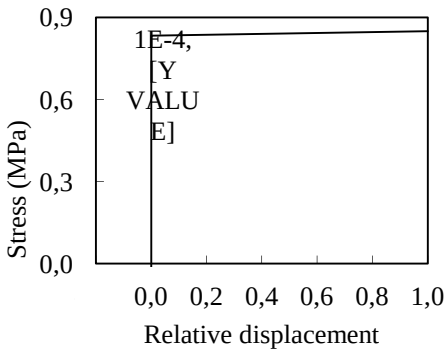

Figure 3: Nonlinear spring function

where

G_{F0} = 0.03 MPa is fracture energy based on max aggregate size of 16 mm.
f_{cmo} = 10 MPa

Table 3: Fracture energy as calculated

Eq.	Value (MN/m)	Difference (%)
1	1.20E-4	0.00
2	1.03E-4	14.43
3	1.25E-4	-3.83
4	1.56E-4	-30.09
5	1.51E-4	-25.78
6	1.52E+2	-26.35

The plastic displacement w_d that governs the compression softening law (Figure 4) was also varied from 0.1 to the value of 0.5 as recommended by [14], [15].

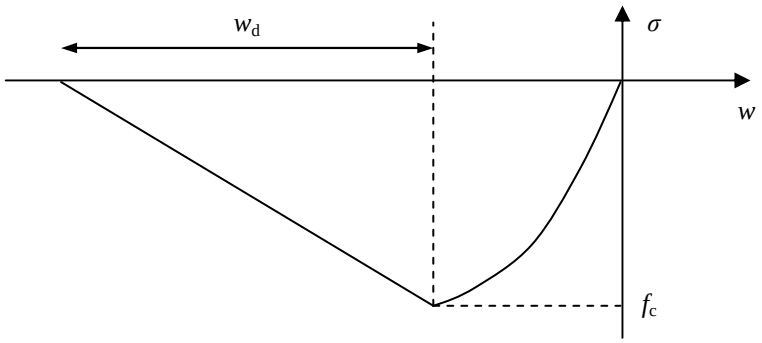

Figure 4: Compression softening law

The last parameter that was varied is the direction of plastic flow β in Drucker-Prager Plasticity Model. The return mapping algorithm for the plastic model is based on predictor-corrector approach as shown in Figure 5 [12]. During the corrector phase of the algorithm in Figure 5, the failure surface moves along the horizontal axis to simulate hardening and softening of concrete. The variation was set from 0 to -0.5. The negative values were set in order to decrease material volume due to crushing [16].

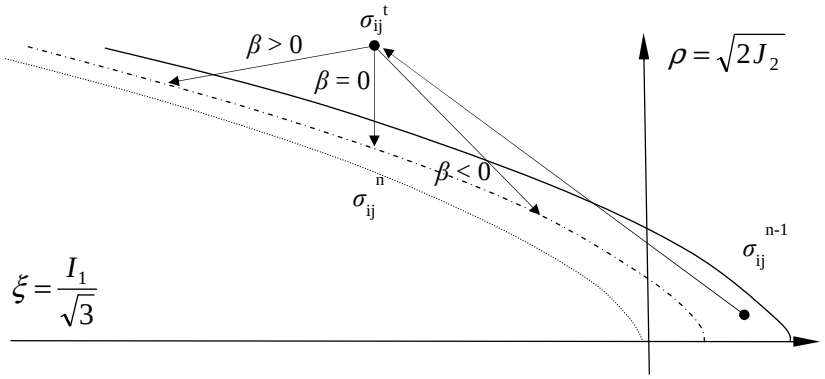

Figure 5: Plastic predictor-corrector algorithm

2.3 Numerical Model

The numerical micromodel was assembled from 3D macro elements (Figure 7a) that represent frame members and 1D truss elements that represent reinforcement bars (Figure 7b). The connection between the rebar and concrete is modelled as perfect as are the connection between frame elements.

Boundary conditions are shown in Figure 7c. Ends of the beam have linear elastic plates with nonlinear area spring and point forces applied. The NL spring opposes the force on the other end of the beam, otherwise it is inactive. Firstly, the foundation support and vertical load is active. The vertical load simulates the weight of the building on the columns. It is implemented in 5 steps with 73 kN increments. After the vertical load is applied fully (365 kN), the column supports in *y* and *z* directions are active and IP loading protocol (Figure 6) is activated. Loading protocol repeats the same force twice (Figure 6).

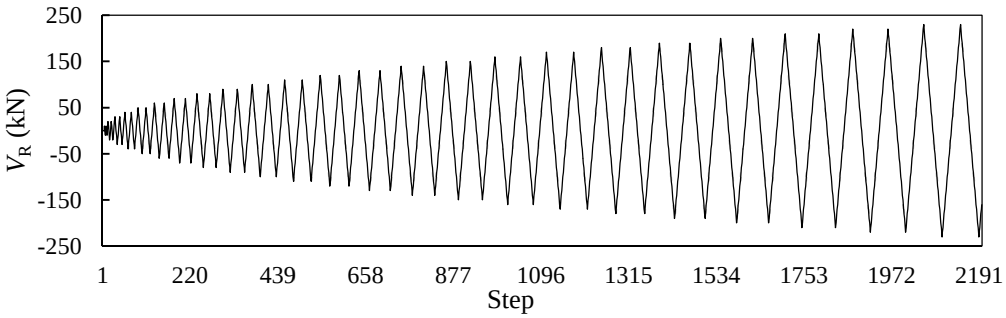

Figure 6: Loading protocol for the numerical model

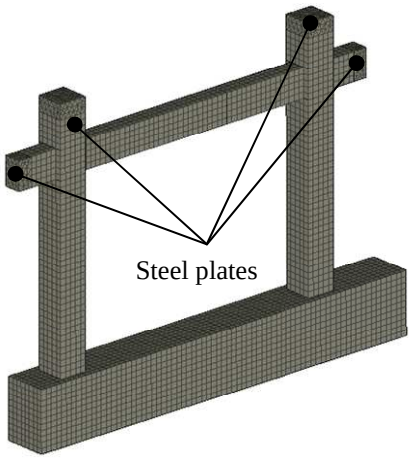

a) Numerical model with FE mesh

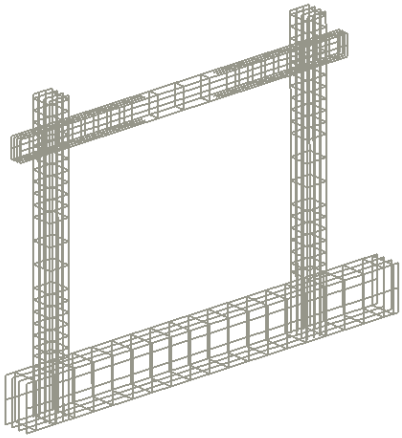

b) Rebar

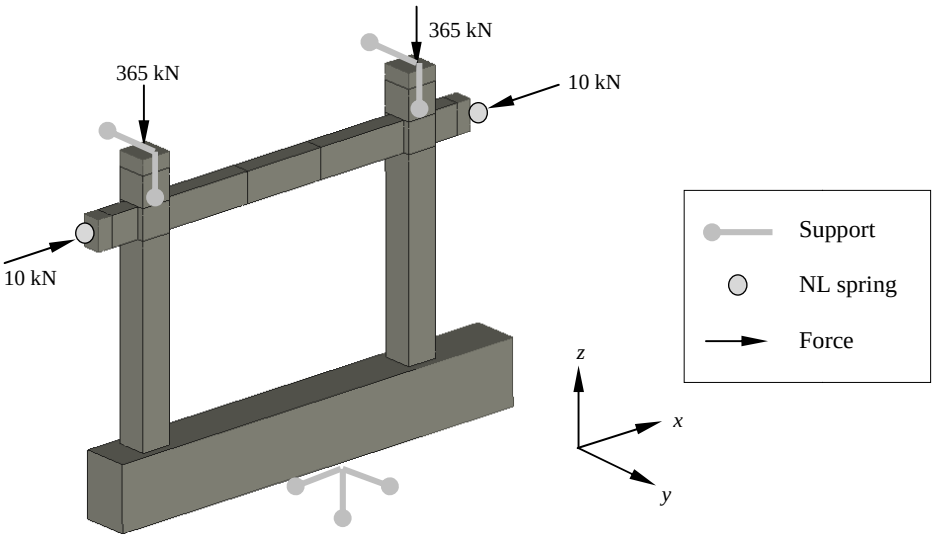

c) Boundary conditions

Figure 7: Numerical model setup

3 Results

Crack patterns both from experimental and numerical studies are shown in Figure 8. The min. crack with was set to hairline width [17].

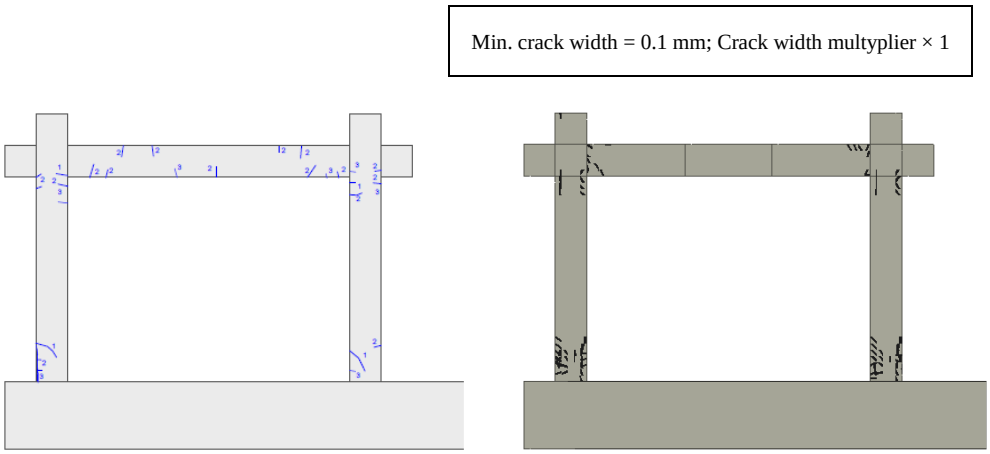

a) Experimental results [4] b) Numerical results

Figure 8: Crack patterns at $d \approx 4$ mm

On Figures 9 - 11 cyclic envelopes are displayed from modified material models. On primary vertical axis shear force vales V_d are plotted, and on primary horizontal axis IP displacements d measured at beams end. On secondary vertical axis, the difference from the maximum shear force V_{max} are plotted. Lastly, on secondary horizontal axis inter-storey drift ratios d_r are plotted. Furthermore, on Figures 2, 9 - 11, the dotted line of the experimental curve annotates monotnoic push of the frame with constant force.

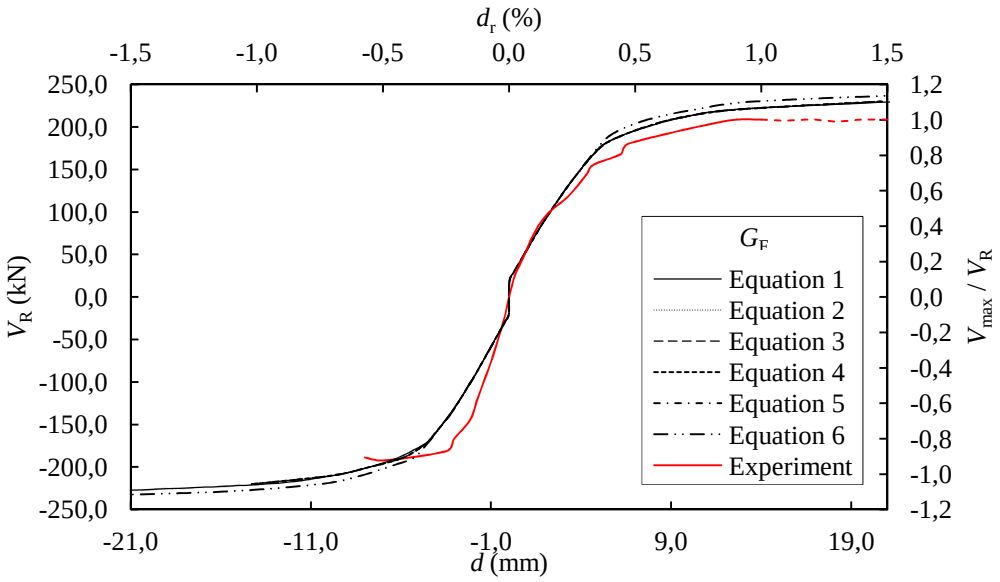

Figure 9: Fracture energy G_f modification

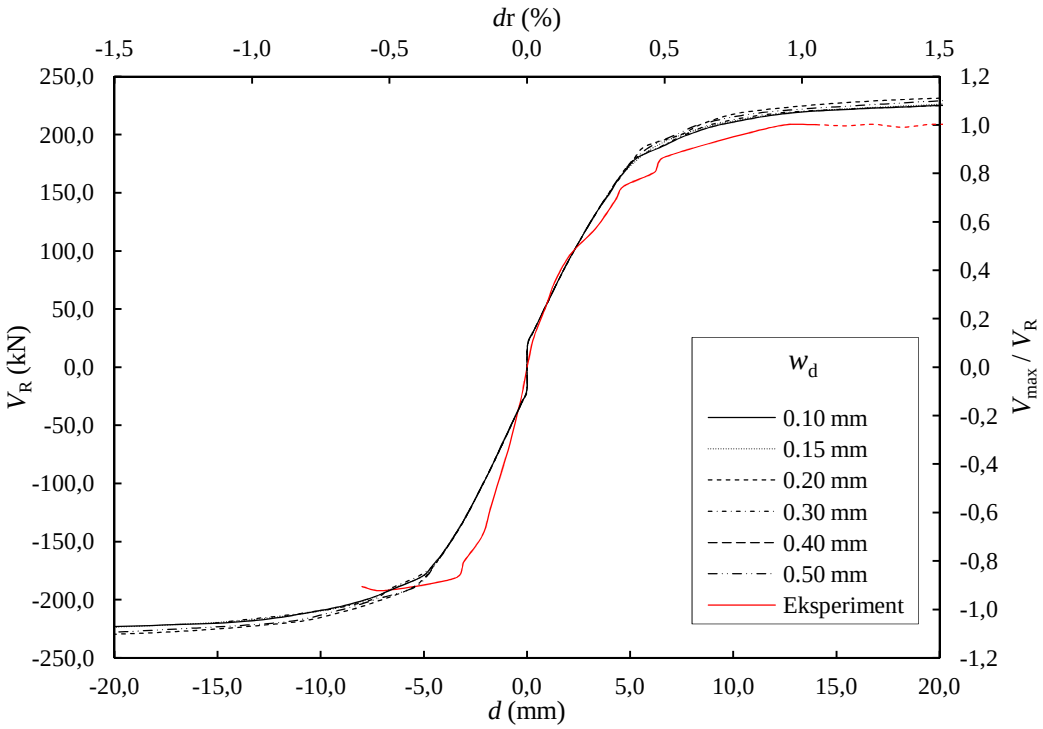

Figure 10: Plastic displacement w_d modification

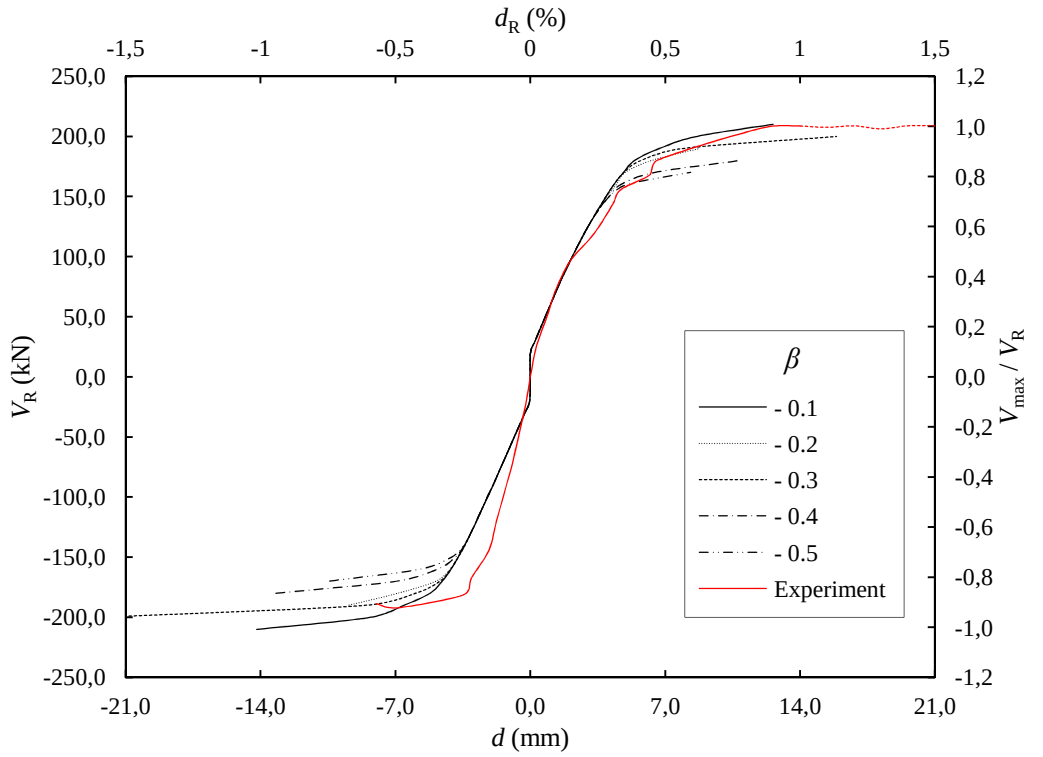

Figure 11: Influence of the direction of plastic flow β

4 Discussion and Conclusions

A 3D FE micromodel of a bare RC frame was developed based on validated 2D micromodel for IP loading. Both model had same material properties and geometry. Yet, the 3D model obtained stronger response in plastic region when compared to its 2D counterpart (Figure 2). Consequently, a calibration of the 3D model was initiated. Calibration involved modifying parameters that govern the plastic behaviour such as: fracture energy (Figure 9), plastic displacement (Figure 10) and direction of the plastic flow (Figure 11).

From the results analysis, it can be concluded that only the direction of plastic flow contributed to lowering of the response. The variations of fracture energy (Figure 9) had non detectable difference except in case of Equation 6, where the response is visibly stronger when compared with other Equations. Likewise, the variations of plastic deformation had only slight effect on modifying the response. Finally, the direction of plastic flow had significant effect on lowering the response. The best fitting value was observed at β = -0.1. Negative number denotes that material volume will decrease due to crushing.

Furthermore, when comparing cracks between experimental and computational model, one can observe that they have similar patterns (Figure 8). Computational model, as expected [18] developed plastic hinges at the lower end of the column and beam – column joint (Figure 8a), as did the experimental specimen (Figure 8a).

In summation, with new value of the direction of plastic flow bare frame model can be considered calibrated in IP direction as well as in OoP direction. Therefore, the computational model can be used in prediction of IP and OoP frame behaviour.

References

[1] P.G. Asteris, L. Cavaleri, F. Di Trapani, A. K. Tsaris, "Numerical modelling of out-of-plane response of infilled frames: State of the art and future challenges for the equivalent strut macromodels", *Engineering Structures*, 2017.

[2] F. Di Trapani *et al.*, "Masonry infills and RC frames interaction : literature overview and state of the art of macromodeling approach", *European Journal of Environmental and Civil Engineering*, **19**(9), 2015.

[3] E. Booth, D. Key, *Earthquake Design Practice for Buildings*. London: Thomas Telford, 2006.

[4] V. Sigmund, D. Penava, "Influence of openings, with and without confinement, on cyclic response of infilled r-c frames — an experimental study", *Journal of Earthquake Engineering*, 18(11): 113–146, 2014.

[5] CEN, *Eurocode 8: Design of Structures for Earthquake Resistance - Part 1: General Rules, Seismic Actions and Rules for Buildings (EN 1998-1:2004)*. Brussels: European Committee for Standardization, 2004.

[6] CEN, *Eurocode 2: Design of concrete structures - Part 1-1: General rules and rules for buildings (EN 1992-1-1:2004)*. Brussels: European Committee for Standardization, 2004.

[7] D. Penava, V. Sarhosis, I. Kožar, I. Guljaš, "Contribution of RC columns and masonry wall to the shear resistance of masonry infilled RC frames containing different in size window and door openings", *Engineering Structures*, **172**: 105–130, 2018.

[8] Cervenka Consulting, “ATENA for Non-Linear Finite Element Analysis of Reinforced Concrete Structures.” Červenka Consulting s.r.o., Prague, 2015.

[9] D. Penava, I. Radić, G. Gazić, V. Sigmund, “Mechanical properties of masonry as required for the seismic resistance verification”, *Technical Gazzette*, **18**(2): 273–280, Jun. 2011.

[10] F. Anić, D. Penava, V. Sarhosis, “Development of a three-dimensional computational model for the in-plane and out-of-plane analysis of masonry-infilled reinforced concrete frames,” in *6th International Conference on Computational Methods in Structural Dynamics and Earthquake Engineering*, 2017.

[11] M.E. Toygar, M. Toparli, F. Sen, M.A. Gungor, “Fracture energy determination and critical crack propagation between core and veneer ceramic interface by experiment and finite element method”, *Materials & Design*, **30**(6): 2278–2282, 2009.

[12] V. Cervenka, L. Jendele, J. Cervenka, *ATENA Program Documentation Part 1 Theory*. Prague: Cervenka Consulting Ltd., 2012.

[13] fib - Fédération internationale du béton, “Code-type models for structural behaviour of concrete: Background of the constitutive relations and material models in the fib Model Code for Concrete Structures 2010”, 2013.

[14] J.G.M. van Mier, “Strain-softening of Concrete under Multiaxial Loading Conditions,” 1984.

[15] R.A. Vonk, “Softening of concrete loaded in compression”, Technische Universiteit Eindhoven, 1992.

[16] J. Cervenka, V. Cervenka, R. Eligehausen, Z. P. Bažant, “Fracture-plastic material model for concrete, application to analysis of powder actuated anchors”, in *Proc. FRAMCOS*, 1998, **3**: 1107–1116, 1998.

[17] J.B. Burland, B.B. Broms, V.F.B. De Mello, “Behaviour of foundations and structures: state-of-the art report”, in *Proc. of the 9th International Conference on Soil Mechanics and Foundation Engineering*, pp. 495–546, 1977.

[18] P.G. Papadopoulos, H. Xenidis, P. Lazaridis, A. Diamantopoulos, P. Lambrou, Y. Arethas, “Achievements of Truss Models for Reinforced Concrete Structures”, *Open J. Civ. Eng.*, **2**(3): 125–131, 2012.